

Glyco-analytical multispecific proteolysis (Glyco-AMP): A simple method for detailed and quantitative glycoproteomic characterization

Serenus Hua, Chloe Y Hu, Bum Jin Kim, Sarah M. Totten, Myung Jin Oh, Nayoung Yun, Charles Chuks Nwosu, Jong Shin Yoo, Carlito B. Lebrilla, and Hyun Joo An

J. Proteome Res., **Just Accepted Manuscript** • DOI: 10.1021/pr400442y • Publication Date (Web): 09 Sep 2013

Downloaded from <http://pubs.acs.org> on September 13, 2013

Just Accepted

“Just Accepted” manuscripts have been peer-reviewed and accepted for publication. They are posted online prior to technical editing, formatting for publication and author proofing. The American Chemical Society provides “Just Accepted” as a free service to the research community to expedite the dissemination of scientific material as soon as possible after acceptance. “Just Accepted” manuscripts appear in full in PDF format accompanied by an HTML abstract. “Just Accepted” manuscripts have been fully peer reviewed, but should not be considered the official version of record. They are accessible to all readers and citable by the Digital Object Identifier (DOI®). “Just Accepted” is an optional service offered to authors. Therefore, the “Just Accepted” Web site may not include all articles that will be published in the journal. After a manuscript is technically edited and formatted, it will be removed from the “Just Accepted” Web site and published as an ASAP article. Note that technical editing may introduce minor changes to the manuscript text and/or graphics which could affect content, and all legal disclaimers and ethical guidelines that apply to the journal pertain. ACS cannot be held responsible for errors or consequences arising from the use of information contained in these “Just Accepted” manuscripts.



1
2
3
4
5
6
7
8
9
10
11
12
13
14
15
16
17
18
19
20
21
22
23
24
25
26
27

Glyco-analytical multispecific proteolysis (Glyco-AMP): A simple method for detailed and quantitative glycoproteomic characterization

28
29
30
31
32
33
34
35
36
37
38
39
40
41
42
43
44
45
46
47
48
49
50
51
52

Serenus Hua,^{1,2} Chloe Y. Hu,³ Bum Jin Kim,¹ Sarah M. Totten,³ Myung Jin Oh,¹
Nayoung Yun,¹ Charles C. Nwosu,³ Jong Shin Yoo,^{1,4} Carlito B. Lebrilla,^{3*†} and
Hyun Joo An^{1,2*†}

- 53
54
55
56
57
58
59
60
1. *Graduate School of Analytical Science and Technology, Chungnam National University, Daejeon, Korea*
 2. *Cancer Research Institute, Chungnam National University, Daejeon, Korea*
 3. *Department of Chemistry, University of California, Davis, CA*
 4. *Division of Mass Spectrometry Research, Korea Basic Science Institute, Ochang, Korea*

* To whom correspondence should be addressed:

Hyun Joo An, email: hjan@cnu.ac.kr, Tel: 82 42-821-8547, Fax: 82 42-821-8551

Carlito B. Lebrilla, email: cblebrilla@ucdavis.edu, Tel: 1 530-752-0504, Fax: 1 530-752-8995

† Hyun Joo An and Carlito B. Lebrilla contributed equally to this paper as co-corresponding authors.

1
2
3
4
5
6
7 **KEYWORDS:** multispecific proteases, non-specific proteases, site-specific glycosylation,
8
9 glycoproteomics, biopharmaceutical glycoproteins, glycan isomers
10

11
12
13 **ABBREVIATIONS:** Glyco-AMP, glyco-analytical multispecific proteolysis; Hex, hexose;
14
15 HexNAc, N-acetylhexosamine; Man, mannose; GlcNAc, N-acetylglucosamine; Fuc, fucose; G1F,
16
17 Hex₄HexNAc₄Fuc; NeuAc, N-acetylneuraminic acid; OAc, O-acetylation
18
19
20
21
22
23
24
25
26
27
28
29
30
31
32
33
34
35
36
37
38
39
40
41
42
43
44
45
46
47
48
49
50
51
52
53
54
55
56
57
58
59
60

ABSTRACT

Despite recent advances, site-specific profiling of protein glycosylation remains a significant analytical challenge for conventional proteomic methodology. To alleviate the issue, we propose glyco-analytical multispecific proteolysis (Glyco-AMP) as a strategy for glycoproteomic characterization. Glyco-AMP consists of rapid, in-solution digestion of an analyte glycoprotein (or glycoprotein mixture) by a multispecific protease (or protease cocktail). Resulting glycopeptides are chromatographically separated by isomer-specific porous graphitized carbon nano-LC, quantified by high-resolution MS, and structurally elucidated by MS/MS. To demonstrate the consistency and customizability of Glyco-AMP methodology, the glyco-analytical performances of multispecific proteases subtilisin, pronase, and proteinase K were characterized in terms of quantitative accuracy, sensitivity, and digestion kinetics. Glyco-AMP was shown to be effective on glycoprotein mixtures as well as glycoproteins with multiple glycosylation sites, providing detailed, quantitative, site- and structure-specific information about protein glycosylation.

INTRODUCTION

Proteins are commonly decorated with long carbohydrate chains, known as glycans, during normal biosynthesis. Over 60% of the known proteome is believed to be glycosylated.¹ As the importance of glycosylation towards protein structure and function becomes ever more apparent, glycomic methods for profiling the detached glycan component of a glycoprotein have undergone extensive innovation and development.²⁻⁴ However, glycoproteomic methods that characterize both glycosylation site and glycan structure are still in their infancy. Until now, the most commonly-used methods have been adapted from traditional proteomics⁵⁻⁷ and often do not sufficiently address the complexities of characterizing a post-translational modification as intricate as glycosylation.

Whereas peptides can be identified and characterized simply by their linear sequence, glycans are branched, with different linkage possibilities between each monosaccharide residue. When peptide and glycan moieties both exist on a single molecule, as with glycopeptides, peptide sequence isomers and glycosylation site isomers further increase the already significant structural complexity.⁸ The abundance of isomeric glycopeptides encountered during glycoproteomic analysis is problematic for mass spectrometry, which cannot distinguish between isomers without the assistance of additional analytical technologies. Consequently, glycoproteomic methods incorporating isomer-specific chromatographic separation and/or tandem MS are crucial for effective glycoprotein characterization.⁹

When analyzing peptides with post-translational modifications such as glycosylation, peptide length must be considered. Large glycopeptides are not only harder to detect by mass spectrometry (due to decreased ionization efficiency as well as instrumental mass limitations) but

1
2
3 can also incorporate multiple glycosylation sites, severely complicating or obfuscating site-
4 specific analysis.¹⁰⁻¹² Proteases with high substrate specificity, such as trypsin, are especially
5
6 prone to creating these large glycopeptides, since their specificity severely limits potential
7
8 cleavage sites.¹³ This is exacerbated by the well-known phenomenon of glycoprotein trypsin
9
10 resistance, wherein large glycosyl modifications sterically hinder protease access to a
11
12 glycoprotein cleavage site, resulting in a missed cleavage.^{14, 15}
13
14
15
16

17
18 While the amino acid sequences of some glycoproteins may be fortuitously rich in tryptic
19
20 cleavage sites, many are not so easily dissected.^{16, 17} The glycoproteomics community is
21
22 therefore in great need of alternative proteases and proteolytic digestion strategies that can be
23
24 broadly applied to enhance and/or replace conventional trypsin-based methodology. One such
25
26 strategy is multispecific (or non-specific) proteolysis, which utilizes proteases or protease
27
28 cocktails with multiple substrate specificities to hydrolyze peptide bonds at a number of different
29
30 sites on a glycoprotein. The resulting digest contains glycopeptides of a roughly consistent size,
31
32 irrespective of the glycoprotein's amino acid sequence or steric hindrance by the glycan moiety.^{18,}
33
34
35

36
37
38
39
40
41
42
43
44
45
46
47
48
49
50
51
52
53
54
55
56
57
58
59
60

19
20
21
22
23
24
25
26
27
28
29
30
31
32
33
34
35
36
37
38
39
40
41
42
43
44
45
46
47
48
49
50
51
52
53
54
55
56
57
58
59
60

Early forays into glycoprotein characterization via multispecific proteolysis involved MS-
only analysis of single glycoprotein digests.²⁰ Sensitivity and specificity were relatively low, due
to interference from ion-suppressing unglycosylated peptides. Later iterations of the strategy
used various chemical methods to immobilize the multispecific proteases on solid supports,
removing a significant amount of the peptide interference originating from protease autolysis.^{21,}
²² However, the most dramatic improvements in glycoproteomics have come just recently, with
the incorporation of nano-LC separation into established mass spectrometric methods.^{8, 9, 23} Use
of nano-LC/MS not only boosts sensitivity by vastly reducing interference from ion-suppressing

1
2
3 peptides, but also enables differentiation of isobaric or even isomeric molecules. Additionally,
4
5 condensation of the in-spectrum dynamic range enables increased use of MS/MS to supplement
6
7 accurate mass MS, adding an extra layer of certainty to glycopeptide identifications.
8
9

10 In this study, isomer-sensitive porous graphitized carbon nano-LC/MS and nano-LC/MS/MS
11
12 are used to interrogate glycopeptide mixtures digested in solution by various multispecific
13
14 proteases. Because the glycoprotein digestions are carried out in solution, rather than by bead-
15
16 immobilized proteases, sample preparation is vastly simplified while experimental variation is
17
18 minimized. Additionally, the in-solution protease digestions inherently proceed faster than bead-
19
20 immobilized protease digestions due to more favorable kinetics.^{24, 25} Though in-solution protease
21
22 digests do contain higher levels of signal-suppressing peptides than immobilized protease digests,
23
24 nano-LC successfully separates the peptide contaminants from the glycopeptide analytes— in
25
26 essence, solving the problem with analytical technology rather than chemical derivatization.
27
28
29
30

31
32 Whereas previous studies have concentrated on the analytical performance of individual
33
34 multispecific proteases, commonly pronase, we demonstrate the general applicability of glyco-
35
36 analytical multispecific proteolysis (Glyco-AMP) by performing detailed and quantitative
37
38 characterization of site-specific protein glycosylation using a variety of multispecific proteases.
39
40 The accuracy and sensitivity of the nano-LC/MS profiling methods are evaluated. Basic
41
42 digestion kinetics and activity of multispecific proteases subtilisin, pronase, and proteinase K are
43
44 tracked and compared. Site-specific glycoform characterization is demonstrated to be effective
45
46 on multiply glycosylated glycoproteins as well as glycoprotein mixtures. Isomer separation by
47
48 porous graphitized carbon nano-LC, combined with MS/MS structural elucidation, reveals fine
49
50 details about the structure and originating site of the glycopeptide.
51
52
53
54
55
56
57
58
59
60

METHODS

Materials and reagents

All multispecific proteases (porcine elastase, papain, porcine pepsin, pronase, proteinase K, subtilisin from *Bacillus licheniformis*, and thermolysin) were obtained from Sigma-Aldrich (St Louis, MO), as were glycoproteins bovine ribonuclease B and human plasma vitronectin. Prostate-specific antigen was obtained from Lee BioSolutions (St Louis, MO). Infliximab was obtained from Janssen Biotech (Horsham, PA). Darbepoetin alfa was obtained from Amgen (Thousand Oaks, CA). Graphitized carbon cartridges were obtained from Grace Davison (Deerfield, IL). Solvents were of LC-MS grade. All other materials and reagents were of analytical grade or higher.

Digestion of glycoproteins by multispecific proteolysis

In general, 50 μg of glycoprotein and 50 μg of protease were dissolved in 100 μL of 100 mM phosphate buffer (pH 7.5) and incubated at 37 $^{\circ}\text{C}$ for 20 minutes. Exceptions occurred during: a) initial protease screening, for which the optimal digestion buffer and temperature for each protease was specified by the manufacturer's product notes; b) kinetics studies, for which multiple digestion timepoints were taken; and c) sensitivity studies, for which the amount of glycoprotein was varied.

Glycopeptide enrichment with graphitized carbon SPE

Digested glycopeptides were enriched by graphitized carbon solid-phase extraction according to previously optimized procedures.²⁶ Briefly, an automated liquid handler (Gilson, Middleton, WI)

1
2
3 conditioned graphitized carbon cartridges with water; loaded aqueous glycopeptide solutions;
4
5 washed with water; then eluted glycopeptides with 40% acetonitrile and 0.05% trifluoroacetic
6
7 acid (v/v) in water. Samples were dried *in vacuo*.
8
9

10 11 12 **Chromatographic separation and MS analysis**

13
14
15 Samples were reconstituted in water and analyzed using an HPLC-Chip Quadrupole Time-of-
16
17 Flight (Chip/Q-TOF) MS system (Agilent Technologies, Santa Clara, CA) comprising an
18
19 autosampler (maintained at 6 °C), capillary pump, nano pump, HPLC-Chip/MS interface, and a
20
21 6520 Q-TOF MS detector. The chip used consisted of a 9 × 0.075 mm i.d. enrichment column
22
23 and a 43 × 0.075 mm i.d. analytical column, both packed with 5 μm porous graphitized carbon as
24
25 the stationary phase, with an integrated nano-ESI spray tip. Chromatographic separation was
26
27 performed according to previously optimized procedures ². Briefly, following sample loading, a
28
29 rapid glycopeptide elution gradient was delivered at 0.4 μL min⁻¹ using solutions of (A) 3.0%
30
31 acetonitrile and 0.1% formic acid (v/v) in water, and (B) 90.0% acetonitrile and 0.5% formic
32
33 acid (v/v) in water, at the following proportions and time points: 5% to 32.8% B, 0 min to 13.3
34
35 min; and 32.8% to 35.9% B, 13.3 min to 16.5 min. The columns were then flushed with 100% B,
36
37 and the analytical column was re-equilibrated with 5% B while the enrichment column was re-
38
39 equilibrated with 0% B. The drying gas temperature was set at 325 °C with a flow rate of 4 L
40
41 min⁻¹ (2 L of filtered nitrogen gas and 2 L of filtered dry compressed air).
42
43
44
45
46
47

48
49 MS spectra were acquired in positive ionization mode over a mass range of *m/z* 500-2000
50
51 with an acquisition time of 1.5 seconds per spectrum. MS/MS spectra were acquired in positive
52
53 ionization mode over a mass range of *m/z* 100-3000 with an acquisition time of 1.5 seconds per
54
55 spectrum. Following an MS scan, precursor compounds were automatically selected for MS/MS
56
57
58
59
60

1
2
3 analysis by the acquisition software based on ion abundance and charge state ($z = 2, 3, \text{ or } 4$) and
4
5 isolated in the quadrupole with a mass bandpass FWHM (full width at half maximum) of $1.3 m/z$.
6
7
8 In general, collision energies for CID fragmentation were calculated for each precursor
9
10 compound based on the following formula:

$$V_{\text{collision}} = 3.6 \text{ V} \left(\frac{m/z}{100 \text{ Da}} \right) - 4.8 \text{ V}$$

11
12
13
14
15
16
17 Here, $V_{\text{collision}}$ is the potential difference across the collision cell. The slope and offset values of
18
19 the energy- m/z ramp could be changed as needed to produce more or less fragmentation.⁸
20
21
22
23

24 **LC/MS data processing and glycopeptide identification**

25
26 After data acquisition, raw LC/MS data was processed using the Molecular Feature Extractor
27
28 algorithm included in the MassHunter Qualitative Analysis software (version B.04.00 SP2,
29
30 Agilent Technologies). MS peaks were filtered with a signal-to-noise ratio of 5.0 and parsed into
31
32 individual ion species. Using expected isotopic distribution, charge state information, and
33
34 retention time, all ion species associated with a single compound (e.g. the doubly protonated ion,
35
36 the triply protonated ion, and all associated isotopologues) were summed together, and the
37
38 neutral mass of the compound was calculated. Using this information, a list of all compound
39
40 peaks in the sample was generated, with abundances represented by chromatographic peak areas.
41
42
43
44

45 Glycopeptides were identified using an in-house software tool based on the GlycoX
46
47 algorithm.²⁷ Taking into account the mass of a potential glycopeptide, the amino acid
48
49 sequence(s) of the protein or proteins it could be derived from, the type of glycosylation (N or O),
50
51 and a given mass tolerance (here, 5 ppm), the algorithm generated a list of potential amino acid
52
53 and glycan compositions associated with a given compound. Results were further filtered based
54
55 on known glycosylation patterns and/or other biological rules.²⁸
56
57
58
59
60

RESULTS AND DISCUSSION

Screening for multispecific proteases with high glycopeptide-generating activity

A number of common, commercially-available proteases were initially screened for their ability to digest glycoproteins into (detectable) glycopeptides. Elastase, papain, pepsin, pronase, proteinase K, subtilisin, and thermolysin were each evaluated by combining 50 μg of protease with 50 μg of well-characterized glycoprotein ribonuclease B (at a total digestion volume of 100 μL). Digestion buffers and conditions were chosen based on the manufacturers' suggested protocols²⁹⁻³⁵— for example, the thermolysin digestion took place at 75 °C in 50 mM Tris and 0.5 mM calcium chloride, while the pepsin digestion took place at 37 °C in 10 mM hydrochloric acid. Digestions were carried out for 20 minutes each, after which the digests were cleaned by graphitized carbon solid-phase extraction and analyzed by nano-LC/MS/MS.

The glycopeptide content of each digest was evaluated by screening MS/MS spectra for glycopeptide-associated fragment ions with m/z 163.06 (Hex+H)⁺, m/z 204.09 (HexNAc+H)⁺, and m/z 366.14 (HexNAc₁Hex₁+H)⁺. Spectra with significant levels (over 50% base peak abundance) of these fragment ions were assumed to be of glycopeptides. The number and ion intensity of glycopeptide spectra were taken as indicative of the number of glycopeptides.

Based on these preliminary evaluations, the subtilisin, pronase, and proteinase K digests were found to contain the highest abundances of glycopeptides. Subtilisin and proteinase K are serine proteases (of bacterial and fungal origin, respectively) that are evolutionarily unrelated yet show a high degree of structural homology, particularly at the catalytic triad.³⁶ Pronase is an enzyme

1
2
3 cocktail of bacterial origin containing mostly serine proteases but also some additional endo- and
4
5 exoproteases. None of these proteases are themselves glycosylated. All are stable over a wide pH
6
7 and temperature range, with optimal activity in slightly alkaline conditions at around 40 °C.
8
9

10 11 12 **Sensitive and quantitative glycoform profiling through multispecific proteolysis** 13 14 15

16
17 To evaluate the quantitative accuracy of Glyco-AMP, subtilisin, pronase, and proteinase K were
18 each applied to analyze bovine ribonuclease B (RNase B). RNase B is a well-characterized
19 glycoprotein with a known glycosylation profile, thus providing a convenient means of
20 validation. The relative abundances of each RNase B glycoform were compared after parallel 20
21 minute digestions by subtilisin, pronase, and proteinase K. Overall profiles in **Figure 1a** are
22 obtained by summing up the abundances of observed glycopeptides associated with each
23 glycoform. To minimize differences in glycopeptide ionization efficiencies, the peptide moieties
24 used for quantitation are kept constant across glycoforms.⁸ High mannose type glycan
25 Man₅GlcNAc₂ (55%) is the most abundant glycan attached to RNase B, followed by
26 Man₆GlcNAc₂ (27%), Man₈GlcNAc₂ (9%), Man₇GlcNAc₂ (7%), and Man₉GlcNAc₂ (3%); these
27 results correlate highly with previous studies quantifying the glycoforms of RNase B.³⁷⁻³⁹ All
28 protease digests result in similar profiles, with the relative abundances of individual glycoforms
29 varying by less than 2% between proteases. For subtilisin, major peptide moieties (exceeding
30 10% abundance) consist of NLTK (66%) and NLT (13%), while the remaining 21% consists of
31 minor peptide moieties SRNL, KSRNL, NL, and SRNLT (in decreasing order of abundance).
32 For pronase, major peptide moieties consist of SRN (52%) and RN (21%), while the remaining
33 27% consists of minor peptide moieties NLT, NLTK, NLTKDR, N, and NL. For proteinase K,
34
35
36
37
38
39
40
41
42
43
44
45
46
47
48
49
50
51
52
53
54
55
56
57
58
59
60

1
2
3 major peptide moieties consist of NLTK (40%), SRNLT (27%), NLT (14%), and SRNL (13%),
4
5 while the remaining 6% consists of minor peptide moieties SRNLTKD and NL. Here, as earlier
6
7 with infliximab, the subtilisin appears to exhibit the highest cleavage specificity (resulting in a
8
9 simpler peptide mixture), while the pronase and proteinase K both exhibit much lower cleavage
10
11 specificity (resulting in a more complex peptide mixture).
12
13
14

15 The sensitivity of Glyco-AMP was also tested by digesting different amounts of RNase B
16
17 with subtilisin. The relative abundances of each RNase B glycoform were compared after
18
19 parallel 20 minute digestions from initial glycoprotein amounts of 10 ng, 100 ng, 1 μg , and 50 μg .
20
21 All initial glycoprotein amounts result in similar profiles, summarized in **Figure 1b**, with the
22
23 relative abundances of individual glycoforms varying by less than 5% between digests. As in
24
25 **Figure 1a**, these results correlate highly with previous studies quantifying the glycoforms of
26
27 RNase B.³⁷⁻³⁹
28
29
30

31 Since RNase B has a molecular weight of approximately 15 kDa, 10 ng of RNase B
32
33 corresponds to 670 femtomoles. Additionally, not all of the sample was injected into the LC/MS
34
35 system— because the autosampler needle could not physically reach the bottom of the sample
36
37 vial, only 8 μL (out of 25 μL) of glycopeptide solution were drawn from the vial for analysis.
38
39 Despite all of this, RNase B glycoform $\text{Man}_9\text{GlcNAc}_2$ was still detected at 5% relative
40
41 abundance, corresponding to the detection (from within a mixture) of just 10 femtomoles of the
42
43 glycoform.
44
45
46
47
48
49
50

51 **Characterization of subtilisin, pronase, and proteinase K enzyme activity**

52
53
54
55
56
57
58
59
60

1
2
3 To better understand the glyco-analytical performance of subtilisin, pronase, and proteinase K,
4 in-depth kinetic studies were performed using infliximab (Remicade®) as a test substrate.
5
6
7
8
9
10
11
12
13
14
15
16
17
18
19
20
21
22
23
24
25
26
27
28
29
30
31
32
33
34
35
36
37
38
39
40
41
42
43
44
45
46
47
48
49
50
51
52
53
54
55
56
57
58
59
60

To better understand the glyco-analytical performance of subtilisin, pronase, and proteinase K, in-depth kinetic studies were performed using infliximab (Remicade®) as a test substrate. Infliximab is a chimeric monoclonal antibody (mAb) made up of a mouse-derived antigen-binding (Fab) region and a human IgG1-derived constant (Fc) region. Glycosylation is present exclusively on the IgG1-derived constant region, and closely imitates (but exhibits some significant differences from) the glycosylation pattern of IgG. Multispecific proteolysis of infliximab is kinetically similar to multispecific proteolysis of pure IgG1 (without interference from IgG isotypes 2-4) or, more relevantly, other mAbs with an IgG1-derived constant region. Thus, the conclusions derived from these experiments may be applied directly to future glycoproteomic analyses of IgG1-derived mAbs such as adalimumab (Humira®), bevacizumab (Avastin®), or rituximab (Rituxan®), all of which possess perfectly conserved IgG1-like amino acid sequences around the N-glycosylation site. These experiments also provide a rough indication of how each protease will perform when applied to glycoproteomic analyses of more complex glycoproteins with multiple glycosylation sites.

To evaluate and characterize each protease, the abundances of the generated glycopeptides were tracked across six time points: 20 min, 60 min, 2 h, 4 h, 8 h, and 18 h. These six time points were tested in each of the three selected proteases: pronase, proteinase K, and subtilisin. All 18 digests were conducted, processed, and analyzed in parallel. Glycopeptides were identified by nano-LC/MS/MS and quantified by nano-LC/MS.

Figure 2 shows the overlaid chromatograms of glycopeptides separated by nano-LC (and identified by accurate mass MS and MS/MS). **Figure 2a** shows the glycopeptides generated by 20 minutes of digestion by subtilisin, whereas **Figure 2b** shows the glycopeptides generated by 18 hours of digestion by subtilisin. These results demonstrate one of the unique advantages of

1
2
3 multispecific proteolysis; that is, the ability to modulate digestion time (as well as enzyme
4 concentration) in order to customize the size or length of the peptide moiety on each
5 glycopeptide.^{21, 22} The 20 minute digestion (**Figure 2a**) results predominantly in longer
6 glycopeptides with peptide moiety sequences of QYNST (the major product) and QYNSTY (a
7 minor product), identifying the originating protein as IgG1-like rather than IgG2-like. Shorter
8 glycopeptides with peptide moiety sequences of NST and NSTY are also present, supporting this
9 identification. In contrast, the 18 hour digestion (**Figure 2b**) results almost entirely in short
10 glycopeptides possessing the NST peptide moiety, with an extremely minor contribution from
11 glycopeptides with a peptide moiety sequence of NSTY.
12
13
14
15
16
17
18
19
20
21
22
23

24
25 **Figure 3** provides a preliminary glimpse of the kinetics of a subtilisin digestion, showing the
26 abundance of glycopeptide QYNST-Hex₄HexNAc₄Fuc (i.e. QYNST-G1F) decreasing over time
27 while the abundance of glycopeptide NST-Hex₄HexNAc₄Fuc (i.e. NST-G1F) increases over time.
28
29
30 **Figure 3b** plots the absolute abundances of these two glycopeptides at six different points during
31 the 18-hour digestion, while **Figures 3a** and **3c** show their chromatograms at these points.
32
33
34
35

36
37 The chromatograms of glycopeptide NST-G1F (**Figure 3c**) highlight the ability of porous
38 graphitized carbon to separate glycopeptide isomers (provided that they are sufficiently small).
39 Here, the only difference between the two glycopeptide isomers is their G1F glycan moiety.
40 Previous glycan structural studies using the same isomer-sensitive porous graphitized carbon
41 stationary phase indicate that on the earlier-eluting G1F isomer, the antennal galactose is
42 attached to the alpha-1,6-linked branch of the glycan, whereas on the later-eluting G1F isomer,
43 the antennal galactose is attached to the alpha-1,3-linked branch.⁴⁰ Based on these results, the
44 predominant G1F isomer present on infliximab is the one in which the antennal galactose is
45 attached to the alpha-1,6-linked branch.
46
47
48
49
50
51
52
53
54
55
56
57
58
59
60

1
2
3 In contrast to glycopeptide NST-G1F, glycopeptide QYNST-G1F (**Figure 3a**) appears to
4 have too long of a peptide moiety for effective isomer separation by porous graphitized carbon
5 nano-LC. However, as mentioned earlier, the presence of a longer peptide moiety (such as
6 QYNST) is still desirable for certain applications because it increases the specificity of the
7 glycosylation site assignment— in this case, by differentiating between IgG isotypes. Detection
8 of glycopeptides with QYNST peptide moieties differentiates glycoforms of infliximab (which is
9 an IgG1 homolog) from glycoforms of IgG2 homologs such as panitumumab (Vectibix®) or
10 denosumab (Prolia®/Xgeva®). In instances of multiply-glycosylated proteins or protein
11 mixtures where multiple sites of glycosylation exist, precise control of peptide moiety length
12 enables researchers to select digestion times that would create glycopeptide markers with high
13 specificity for a particular site of glycosylation. These markers could then be used to quantify
14 selected glycoforms of a specific glycoprotein, with implications for biosimilar batch analysis or
15 biomarker research.

16
17
18
19
20
21
22
23
24
25
26
27
28
29
30
31
32
33
34 **Figure 4** tracks the progression over time of infliximab digestion by subtilisin (**Figure 4a**),
35 pronase (**Figure 4b**), and proteinase K (**Figure 4c**). For each digestion timepoint, the percent
36 contributions of each peptide moiety to the overall glycopeptide population are plotted. These
37 charts may be used to estimate the rate of glycopeptide production at a given time point and can
38 help optimize a digestion for generation of a target glycopeptide.

39
40
41
42
43
44
45
46 In subtilisin (**Figure 4a**), as discussed earlier, the major peptide moieties are initially
47 QYNST and NST, with minor contributions from QYNSTY and NSTY. As the digestion
48 progresses, abundances of QYNST and QYNSTY drop drastically, eventually becoming
49 undetectable, while abundances of NST rise correspondingly. However, the contribution from
50 NSTY is more interesting. For the first two hours of the digestion, abundances of NSTY rise,
51
52
53
54
55
56
57
58
59
60

1
2
3 very nearly imitating the reaction plot of NST (proportionately, at much lower levels). However,
4
5 after the first two hours, abundances of NSTY drop, more closely imitating the reaction plots of
6
7 QYNST and QYNSTY. Presumably, the initial rise is fed largely by digestion of QYNSTY
8
9 peptide moieties (or even larger precursors) to form NSTY. Simultaneously, NSTY peptide
10
11 moieties are being digested to form NST. Approximately two hours later, the rate of NSTY
12
13 formation slows (due to lack of substrate) and is overtaken by the rate of NSTY digestion,
14
15 resulting in the observed decreases in abundance of NSTY peptide moieties. By the 18 hour
16
17 digestion timepoint, 96% of all infliximab glycopeptides have NST peptide moieties, while the
18
19 remaining 4% have NSTY peptide moieties. During the observed course of the reaction, total
20
21 detected glycopeptide abundances (in ion counts) increase only slightly, by just 4%, indicating
22
23 that, after the 20 minute timepoint, subtilisin is mainly acting on already-digested short
24
25 glycopeptides, and very little undigested infliximab remains.
26
27
28
29
30

31
32 In pronase (**Figure 4b**), the major peptide moieties are initially NST and YNST, with minor
33
34 contributions from TKPREEQYNST and EEQYNST. As the digestion progresses, abundances
35
36 of TKPREEQYNST and EEQYNST drop drastically; abundances of YNST decrease at a slower
37
38 rate; and abundances of NST increase correspondingly. The slower rate of decrease for YNST
39
40 peptide moieties may be due in part to digestion of TKPREEQYNST and EEQYNST to form
41
42 new YNST; however, abundances of YNST appears to decrease quite slowly even after
43
44 abundances of TKPREEQYNST and EEQYNST peptide moieties have dropped below
45
46 detectable levels. A more likely explanation is that, due to enzyme autolysis, the pronase is
47
48 losing activity as the digestion progresses. This would explain the lack of significant decreases in
49
50 YNST abundances (as well as the lack of corresponding increases in NST abundances) after the
51
52 four hour digestion timepoint. Even after 18 hours of digestion by pronase, only 84% of all
53
54
55
56
57
58
59
60

1
2
3
4
5
6
7
8
9
10
11
12
13
14
15
16
17
18
19
20
21
22
23
24
25
26
27
28
29
30
31
32
33
34
35
36
37
38
39
40
41
42
43
44
45
46
47
48
49
50
51
52
53
54
55
56
57
58
59
60

infliximab glycopeptides have NST peptide moieties, while the remaining 16% have YNST peptide moieties. During the observed course of the reaction, total detected glycopeptide abundances (in ion counts) increase only slightly, by just 8%, indicating that, after the 20 minute timepoint, pronase is mainly acting on already-digested short glycopeptides, and very little undigested infliximab remains.

In proteinase K (**Figure 4c**), the major peptide moieties are initially QYNST, TKPREEQYNST, and NST, with a minor contribution from YNST. As the digestion progresses, abundances of QYNST and TKPREEQYNST generally decrease, while abundances of NST and YNST generally increase. Due to the curious behavior of the digestion during the initial two hours, additional timepoints have been added to the analysis. In all, timepoints are shown for 20 min, 40 min, 60 min, 90 min, 2 h, 3 h, 4 h, 6 h, 8 h, 12 h, and 18 h of digestion.

In contrast to the subtilisin and pronase digestions, total detected glycopeptide abundances (in ion counts) increase dramatically, by 150%, during the initial two hours of the proteinase K digestion, indicating that proteinase K is still digesting either whole infliximab or large pieces thereof up until this timepoint. After two hours, there are no further increases in total detected glycopeptide abundance, indicating that from this timepoint on, proteinase K is mainly acting on already-digested short glycopeptides, and that very little undigested infliximab remains.

The initial rise in abundance of QYNST and TKPREEQYNST peptide moieties is most likely related to the continuing digestion of whole infliximab during this period. After two hours, all of the whole infliximab has been digested into (glyco)peptides of various sizes, and abundances of QYNST and TKPREEQYNST begin to drop. Correspondingly, the rate of generation of NST and YNST peptide moieties increases. After 18 hours of digestion by proteinase K, the rate of change has slowed, but not stopped. The dominant peptide moiety at

1
2
3 this time is NST, comprising 89% of all infliximab glycopeptides; however, detectable
4 abundances of YNST (8%) and QYNST (3%) peptide moieties are still present.
5
6

7
8 When selecting the appropriate multispecific protease for an application, sensitivity may also
9 be a consideration. Total detected glycopeptide abundances (in ion counts) were used to evaluate
10 the yield, and thus sensitivity, afforded by each protease digest. For subtilisin, the total detected
11 glycopeptide abundance was 4.2×10^7 counts at 20 minutes, increasing to 4.4×10^7 counts by
12 the end of the digestion. For pronase, the total detected glycopeptide abundance was 7.7×10^7
13 counts at 20 minutes, increasing to 8.4×10^7 counts by the end of the digestion. For proteinase K,
14 the total detected glycopeptide abundance was 1.0×10^7 counts at 20 minutes, increasing rapidly
15 to 2.5×10^7 counts after two hours and remaining steady until the end of the digestion.
16
17
18
19
20
21
22
23
24
25
26

27 When determining the optimal digestion conditions for a particular application, multiple
28 factors come into play. Specificity of the peptide moiety for a single site of glycosylation;
29 digestion yield (i.e. sensitivity); and digestion purity (i.e. the degree of signal splitting) should all
30 be considered. For example, at the 18 hour digestion timepoints in **Figure 4**, all three proteases
31 offer their own unique advantages. Proteinase K (**Figure 4c**) offers the highest degree of
32 glycosite specificity, since the digest contains glycopeptides with three overlapping peptide
33 moieties, two of which cross-confirm that the originating IgG-like protein is homologous to the
34 IgG1 isotype, rather than the IgG2 isotype. Pronase (**Figure 4b**) offers the highest glycopeptide
35 yield, increasing the sensitivity of the analysis and decreasing the amount of analyte glycoprotein
36 necessary. Subtilisin (**Figure 4a**) offers the highest glycopeptide purity, with almost all of the
37 glycopeptides condensed to a single peptide moiety, geometrically reducing the complexity of
38 the digest. Depending on the specific application, researchers have an unlimited menu of options
39 with which to customize their Glyco-AMP digestion conditions for optimal results.
40
41
42
43
44
45
46
47
48
49
50
51
52
53
54
55
56
57
58
59
60

Site-specific profiling with protein mixtures and multiple glycosylation sites

The main purpose of using multispecific proteolysis to digest glycoproteins is to obtain site-specific information about their glycosylation, particularly when there is more than one glycosylation site involved. This can occur when more than one glycoprotein is present in a mixture (e.g. as a result of co-precipitation or co-elution); or, when a glycoprotein has multiple glycosylation sites. In-solution multispecific proteolysis is demonstrated to be effective in both of these scenarios.

Figure 5 shows the chromatograms of glycopeptides digested by subtilisin from a mixture of RNase B and prostate-specific antigen (PSA). PSA is a commonly-used clinical biomarker for prostate cancer;^{41, 42} however, in recent years, its specificity has been called into question.^{43, 44} Closer examination of its glycosylation may provide a means of increasing the specificity of PSA as a biomarker. Unfortunately, since PSA is present at relatively low levels in serum, isolation by either immunoprecipitation or chromatography may well result in contamination by co-precipitating or co-eluting proteins, necessitating site-specific analysis to confirm the origin of glycosylation. Here, site-specific peptide moieties unambiguously identify each glycopeptide as originating from either RNase B or PSA. PSA glycoforms detected during this analysis (**Figure 6**) support and expand upon previous studies of PSA glycosylation.^{45, 46} For example, multiple regioisomeric glycoforms of PSA are baseline-resolved by porous graphitized carbon nano-LC, providing structural specificity to the analysis. These regioisomers most likely arise from differential linkages of the terminal sialic acids (which can be either alpha-2,3- or alpha-2,6-

1
2
3 linked to the preceding galactoses) and may be confirmed in future experiments by linkage-
4 specific glycosidase digestion.⁴⁰
5
6

7
8 Pronase digestion of vitronectin, a glycoprotein with three sites of glycosylation, reveals the
9 detailed glycosylation profile shown in **Figure 7**. Recent research has indicated that vitronectin,
10 an abundant serum glycoprotein, may be involved in the early stages of cancer.^{47, 48} However,
11 few studies have examined vitronectin glycosylation,⁴⁹ and none have been able to isolate
12 glycoforms at specific sites of glycosylation until now. Part of the difficulty may have to do with
13 the proteomics community's traditional reliance on trypsin— three of vitronectin's glycosylation
14 sites are located in the near vicinity of tryptic cleavage sites, with two in a P1' position,
15 immediately adjacent to a tryptic cleavage site, and another one located in a P2' position. Steric
16 hindrance of trypsin at these sites would cause missed cleavages, leading to excessively large
17 glycopeptides that would be difficult to detect or characterize.
18
19
20
21
22
23
24
25
26
27
28
29
30

31
32 In **Figure 7**, multispecific proteolysis is employed to sidestep the issue by creating
33 glycopeptides that are small enough for easy detection as well as isomeric separation by porous
34 graphitized carbon nano-LC, yet still retain their specificity for a single site of glycosylation. For
35 each site of glycosylation, glycan occupation was confirmed by at least two overlapping peptide
36 moieties. For ⁸⁶Asn, glycopeptides were detected with peptide moieties NN (91%), NNAT (6%),
37 and NAT (3%). For ¹⁶⁹Asn, glycopeptides were detected with peptide moieties NGS (89%) and
38 KNKS (3%). For ²⁴²Asn, glycopeptides were detected with peptide moieties NISDG (79%) and
39 NIS (21%). Multiple regioisomeric glycan moieties, arising from differences in either
40 monosaccharide linkage or position, were chromatographically separated and differentiated;
41 however, *de novo* identification was not possible based on CID MS/MS data alone. As this is the
42 first site-specific analysis of vitronectin glycosylation with any kind of isomer separation, further
43
44
45
46
47
48
49
50
51
52
53
54
55
56
57
58
59
60

1
2
3 experimentation with linkage-specific glycosidases (or other structural elucidation methods) will
4
5 be necessary in order to determine the exact structural characteristics of the isomeric glycoforms.
6
7
8
9

10 **Isomer-specific LC/MS/MS characterization of site-specific glycoforms**

11
12
13
14

15 One of the major advantages of multispecific proteolysis is its ability to generate small
16
17 glycopeptides that can be isomerically separated by nano-LC and then structurally characterized
18
19 by MS/MS. **Figure 8** further explores this concept by displaying isomer-specific MS/MS spectra
20
21 of two chromatographically separated O-glycopeptide isomers originating from a pronase digest
22
23 of darbepoetin alfa (aka novel erythropoiesis stimulating protein, or NESP). Darbepoetin alfa is a
24
25 commonly-used biotherapeutic analogue of erythropoietin, the glycoprotein that stimulates red
26
27 blood cell production.
28
29
30

31 The glycopeptide isomers in **Figure 8** are each comprised of a tri-O-acetylated
32
33 Hex₁HexNAc₁NeuAc₂ O-glycan moiety attached to peptide moiety SPPDAASAAP. Extensive
34
35 CID fragmentation of both the glycan and peptide moieties not only confirms the composition of
36
37 the glycopeptides, but also reveals stark differences in the MS/MS fingerprint of each isomer.
38
39 For example, the fragments at m/z 204.09 (HexNAc+H)⁺, m/z 274.09 (NeuAc-H₂O+H)⁺, m/z
40
41 292.10 (NeuAc+H)⁺, m/z 366.14 (Hex₁HexNAc₁+H)⁺, m/z 657.23 (Hex₁HexNAc₁NeuAc₁+H)⁺,
42
43 and m/z 1461.62 (SPPDAASAAP+HexNAc₁NeuAc₁+2OAc+H)⁺ are present in high abundance
44
45 in MS/MS of the isomer eluting at 14.5 minutes (**Figure 8a**), yet conspicuously absent in
46
47 MS/MS of the isomer eluting at 15.6 minutes (**Figure 8b**).
48
49
50
51
52

53 Closer examination suggests that discrepancies between the isomers in **Figures 8a** and **8b**
54
55 stem from differing degrees of O-acetylation on their sialic acids. In **Figure 8a**, the fragments at
56
57
58
59
60

1
2
3 m/z 1461.62 (SPPDAASAAP+HexNAc₁NeuAc₁+2OAc+H)⁺ and m/z 1346.54
4
5 (SPPDAASAA+HexNAc₁NeuAc₁+2OAc+H)⁺ suggest the *HexNAc*-attached NeuAc as the site
6
7 of two out of three total O-acetyl modifications on this isomer. These fragments are completely
8
9 absent from **Figure 8b**; however, **Figure 8b** does show a high abundance of the fragment at m/z
10
11 538.18 (Hex₁NeuAc₁+2OAc+H)⁺, which conversely suggests the *Hex*-attached NeuAc as the site
12
13 of two out of three total O-acetyl modifications on this isomer. Based on these data, we propose
14
15 that the isomer shown in **Figure 8a** has one O-acetyl modification on the Hex-attached NeuAc
16
17 and two O-acetyl modifications on the HexNAc-attached NeuAc, while the isomer shown in
18
19 **Figure 8b** has two O-acetyl modifications on the Hex-attached NeuAc and one O-acetyl
20
21 modification on the HexNAc-attached NeuAc.
22
23
24
25
26

27 Previous studies of darbepoetin alfa glycosylation have found a maximum of two O-acetyl
28
29 modifications per sialic acid for both N- and O-glycosylation,^{50, 51} in concurrence with the
30
31 proposed structures for the two isomers shown here. Of course, additional structural differences
32
33 are also possible between these two isomers— for instance, either of the two sialic acids on each
34
35 glycopeptide might be connected to the rest of the molecule by a different linkage.
36
37 Complementary structural elucidation methods such as exoglycosidase digestion and/or non-
38
39 ergodic MS/MS may provide further information.^{52, 53}
40
41
42

43 O-acetylation increases the half-life and potency of recombinant erythropoietins by
44
45 interfering with *in vivo* enzymatic desialylation of the glycans present on the drug.⁵⁴ Additionally,
46
47 O-acetylated sialic acids act as binding substrates for several viruses, including common cold
48
49 viruses such as influenza C as well as certain coronaviruses.^{55, 56} Thus, the level of fine structural
50
51 detail provided by nano-LC/MS/MS of multispecific protease digests could be of great import to
52
53 both producers and regulators of biopharmaceutical drugs and vaccines.
54
55
56
57
58
59
60

CONCLUSION

Though subtilisin, pronase, and proteinase K have previously been described as "non-specific" proteases, detailed and extensive characterization reveals that these proteases neither lack specificity, nor digest proteins at random. Instead, they may best be described as "multispecific" proteases, possessing multiple substrate specificities, such that they hydrolyze peptide bonds at a large, but finite number of sites on a (glyco)protein. As demonstrated, the interplay of these different substrate specificities can be analytically exploited to optimize glycoprotein digestion and glycopeptide generation, providing a valuable new class of tools for the burgeoning field of glycoproteomics.

Analogously to the thousands of restriction enzymes available to genomicists, a large protease toolbox provides greater flexibility and experimental customizability to the field of proteomics, and particularly to the characterization of post-translational modifications such as glycosylation. Glyco-AMP packages this flexibility into a rapid, easy-to-use methodology that can be broadly applied to a variety of complex glycoproteins as well as glycoprotein mixtures. Using the simple, in-solution digestion protocol, researchers avoid laborious protease immobilization reactions while increasing quantitative reproducibility. In addition, researchers can control peptide moiety length by adjusting the multispecific digestion kinetics, allowing them to choose the degrees of glycosylation site specificity and glycan structure specificity necessary for their experiment.

Multispecific proteases, as well as the glyco-AMP strategy in general, find maximum utility in detailed, structure-specific studies of the glycoproteome. In contrast to trypsin, which is most

1
2
3 effective at sketching an outline of whole glycoproteomes, glyco-AMP and related strategies are
4 crucial for filling in the fine details about specific targeted glycoproteins or mixtures. As a result,
5 glyco-AMP is an ideal method for detailed characterization of potential glycoprotein biomarkers
6 as well as glycosylated biopharmaceutical products, providing unparalleled site- and structure-
7 specific information.
8
9
10
11
12
13
14
15
16

17 **ACKNOWLEDGMENTS**

18
19
20 We are grateful for the support provided by the 2012 University-Institute Cooperation Program
21 via the National Research Foundation of Korea as well as the Converging Research Center
22 Program (2012K001505 for H. J. An) via the Ministry of Education, Science and Technology.
23
24
25
26
27
28
29
30
31
32
33
34
35
36
37
38
39
40
41
42
43
44
45
46
47
48
49
50
51
52
53
54
55
56
57
58
59
60

REFERENCES

1. Apweiler, R.; Hermjakob, H.; Sharon, N., On the frequency of protein glycosylation, as deduced from analysis of the SWISS-PROT database. *Biochimica et Biophysica Acta (BBA) - General Subjects* **1999**, 1473, (1), 4-8.
2. Hua, S.; Williams, C. C.; Dimapasoc, L. M.; Ro, G. S.; Ozcan, S.; Miyamoto, S.; Lebrilla, C. B.; An, H. J.; Leiserowitz, G. S., Isomer-Specific Chromatographic Profiling Yields Highly Sensitive And Specific Potential N-Glycan Biomarkers For Epithelial Ovarian Cancer. *J Chromatogr A* **2013**, (0).
3. Hua, S.; An, H. J.; Ozcan, S.; Ro, G. S.; Soares, S.; DeVere-White, R.; Lebrilla, C. B., Comprehensive native glycan profiling with isomer separation and quantitation for the discovery of cancer biomarkers. *Analyst* **2011**, 136, (18), 3663-3671.
4. Hua, S.; Lebrilla, C.; An, H. J., Application of nano-LC-based glycomics towards biomarker discovery. *Bioanalysis* **2011**, 3, (22), 2573-2585.
5. Ahn, Y.; Shin, P.; Ji, E.; Kim, H.; Yoo, J., A lectin-coupled, multiple reaction monitoring based quantitative analysis of human plasma glycoproteins by mass spectrometry. *Analytical and Bioanalytical Chemistry* **2012**, 402, (6), 2101-2112.
6. Miyoshi, E.; Nakano, M., Fucosylated haptoglobin is a novel marker for pancreatic cancer: Detailed analyses of oligosaccharide structures. *PROTEOMICS* **2008**, 8, (16), 3257-3262.
7. Kurogochi, M.; Amano, M.; Fumoto, M.; Takimoto, A.; Kondo, H.; Nishimura, S.-I., Reverse Glycoblotting Allows Rapid-Enrichment Glycoproteomics of Biopharmaceuticals and Disease-Related Biomarkers. *Angewandte Chemie International Edition* **2007**, 46, (46), 8808-8813.

- 1
2
3
4
5
6
7
8
9
10
11
12
13
14
15
16
17
18
19
20
21
22
23
24
25
26
27
28
29
30
31
32
33
34
35
36
37
38
39
40
41
42
43
44
45
46
47
48
49
50
51
52
53
54
55
56
57
58
59
60
8. Hua, S.; Nwosu, C.; Strum, J.; Seipert, R.; An, H.; Zivkovic, A.; German, J. B.; Lebrilla, C., Site-specific protein glycosylation analysis with glycan isomer differentiation. *Anal Bioanal Chem* **2012**, 403, (5), 1291-1302.
 9. Hua, S.; An, H. J., Glycoscience aids in biomarker discovery. *BMB Rep* **2012**, 45, (6), 323-30.
 10. Dallas, D. C.; Martin, W. F.; Hua, S.; German, J. B., Automated glycopeptide analysis—review of current state and future directions. *Briefings in Bioinformatics* **2012**.
 11. Kim, J. Y.; Kim, S.-K.; Kang, D.; Moon, M. H., Dual Lectin-Based Size Sorting Strategy to Enrich Targeted N-Glycopeptides by Asymmetrical Flow Field-Flow Fractionation: Profiling Lung Cancer Biomarkers. *Analytical Chemistry* **2012**, 84, (12), 5343-5350.
 12. Schlosser, A.; Vanselow, J. T.; Kramer, A., Mapping of Phosphorylation Sites by a Multi-Protease Approach with Specific Phosphopeptide Enrichment and NanoLC-MS/MS Analysis. *Analytical Chemistry* **2005**, 77, (16), 5243-5250.
 13. Pompach, P.; Chandler, K. B.; Lan, R.; Edwards, N.; Goldman, R., Semi-Automated Identification of N-Glycopeptides by Hydrophilic Interaction Chromatography, nano-Reverse-Phase LC-MS/MS, and Glycan Database Search. *Journal of Proteome Research* **2012**, 11, (3), 1728-1740.
 14. Wu, Z. L.; Ethen, C.; Hickey, G. E.; Jiang, W., Active 1918 pandemic flu viral neuraminidase has distinct N-glycan profile and is resistant to trypsin digestion. *Biochemical and Biophysical Research Communications* **2009**, 379, (3), 749-753.
 15. Fujihara, J.; Yasuda, T.; Kunito, T.; Fujii, Y.; Takatsuka, H.; Moritani, T.; Takeshita, H., Two N-Linked Glycosylation Sites (Asn18 and Asn106) Are Both Required for Full Enzymatic Activity, Thermal Stability, and Resistance to Proteolysis in Mammalian

- 1
2
3 Deoxyribonuclease I. *Bioscience, Biotechnology, and Biochemistry* **2008**, 72, (12), 3197-
4
5 3205.
6
7
8 16. Giménez, E.; Ramos-Hernan, R.; Benavente, F.; Barbosa, J.; Sanz-Nebot, V., Analysis of
9
10 recombinant human erythropoietin glycopeptides by capillary electrophoresis electrospray-
11
12 time of flight-mass spectrometry. *Analytica Chimica Acta* **2012**, 709, (0), 81-90.
13
14
15 17. Wang, D.; Hincapie, M.; Rejtar, T.; Karger, B. L., Ultrasensitive Characterization of Site-
16
17 Specific Glycosylation of Affinity-Purified Haptoglobin from Lung Cancer Patient Plasma
18
19 Using 10 μm i.d. Porous Layer Open Tubular Liquid Chromatography-Linear Ion Trap
20
21 Collision-Induced Dissociation/Electron Transfer Dissociation Mass Spectrometry.
22
23 *Analytical Chemistry* **2011**, 83, (6), 2029-2037.
24
25
26
27 18. Swaney, D. L.; Wenger, C. D.; Coon, J. J., Value of Using Multiple Proteases for Large-
28
29 Scale Mass Spectrometry-Based Proteomics. *Journal of Proteome Research* **2010**, 9, (3),
30
31 1323-1329.
32
33
34 19. Seipert, R. R.; Dodds, E. D.; Lebrilla, C. B., Exploiting Differential Dissociation Chemistries
35
36 of O-Linked Glycopeptide Ions for the Localization of Mucin-Type Protein Glycosylation.
37
38 *Journal of Proteome Research* **2008**, 8, (2), 493-501.
39
40
41 20. An, H. J.; Peavy, T. R.; Hedrick, J. L.; Lebrilla, C. B., Determination of N-Glycosylation
42
43 Sites and Site Heterogeneity in Glycoproteins. *Analytical Chemistry* **2003**, 75, (20), 5628-
44
45 5637.
46
47
48 21. Clowers, B. H.; Dodds, E. D.; Seipert, R. R.; Lebrilla, C. B., Site Determination of Protein
49
50 Glycosylation Based on Digestion with Immobilized Nonspecific Proteases and Fourier
51
52 Transform Ion Cyclotron Resonance Mass Spectrometry. *Journal of Proteome Research*
53
54 **2007**, 6, (10), 4032-4040.
55
56
57
58
59
60

- 1
2
3
4
5
6
7
8
9
10
11
12
13
14
15
16
17
18
19
20
21
22
23
24
25
26
27
28
29
30
31
32
33
34
35
36
37
38
39
40
41
42
43
44
45
46
47
48
49
50
51
52
53
54
55
56
57
58
59
60
22. Dodds, E. D.; Seipert, R. R.; Clowers, B. H.; German, J. B.; Lebrilla, C. B., Analytical Performance of Immobilized Pronase for Glycopeptide Footprinting and Implications for Surpassing Reductionist Glycoproteomics. *Journal of Proteome Research* **2008**, 8, (2), 502-512.
23. Froehlich, J. W.; Barboza, M.; Chu, C.; Lerno, L. A.; Clowers, B. H.; Zivkovic, A. M.; German, J. B.; Lebrilla, C. B., Nano-LC-MS/MS of Glycopeptides Produced by Nonspecific Proteolysis Enables Rapid and Extensive Site-Specific Glycosylation Determination. *Analytical Chemistry* **2011**, 83, (14), 5541-5547.
24. He, P.; Greenway, G.; Haswell, S., Development of enzyme immobilized monolith micro-reactors integrated with microfluidic electrochemical cell for the evaluation of enzyme kinetics. *Microfluid Nanofluid* **2010**, 8, (5), 565-573.
25. Calleri, E.; Temporini, C.; Gasparrini, F.; Simone, P.; Villani, C.; Ciogli, A.; Massolini, G., Immobilized trypsin on epoxy organic monoliths with modulated hydrophilicity: Novel bioreactors useful for protein analysis by liquid chromatography coupled to tandem mass spectrometry. *Journal of Chromatography A* **2011**, 1218, (49), 8937-8945.
26. Kronewitter, S. R.; de Leoz, M. L. A.; Peacock, K. S.; McBride, K. R.; An, H. J.; Miyamoto, S.; Leiserowitz, G. S.; Lebrilla, C. B., Human Serum Processing and Analysis Methods for Rapid and Reproducible N-Glycan Mass Profiling. *Journal of Proteome Research* **2010**, 9, (10), 4952-4959.
27. An, H. J.; Tillinghast, J. S.; Woodruff, D. L.; Rocke, D. M.; Lebrilla, C. B., A New Computer Program (GlycoX) To Determine Simultaneously the Glycosylation Sites and Oligosaccharide Heterogeneity of Glycoproteins. *Journal of Proteome Research* **2006**, 5, (10), 2800-2808.

- 1
2
3
4 28. Kronewitter, S. R.; An, H. J.; de Leoz, M. L.; Lebrilla, C. B.; Miyamoto, S.; Leiserowitz, G.
5
6 S., The development of retrosynthetic glycan libraries to profile and classify the human
7
8 serum N-linked glycome. *PROTEOMICS* **2009**, 9, (11), 2986-2994.
9
- 10 29. Bieth, J.; Spiess, B.; Wermuth, C. G., The synthesis and analytical use of a highly sensitive
11
12 and convenient substrate of elastase. *Biochemical Medicine* **1974**, 11, (4), 350-357.
13
- 14 30. Glazer, A. N.; Smith, E. L., 14 Papain and Other Plant Sulfhydryl Proteolytic Enzymes. In
15
16 *The Enzymes*, Paul, D. B., Ed. Academic Press: 1971; Vol. Volume 3, pp 501-546.
17
- 18 31. Ryle, A., Pepsins, gastricsins and their zymogens. *Methods of enzymatic analysis* **1984**, 228-
19
20 21
22 233.
23
- 24 32. Juhasz, P.; Martin, S. A., The utility of nonspecific proteases in the characterization of
25
26 glycoproteins by high-resolution time-of-flight mass spectrometry. *International Journal of*
27
28 *Mass Spectrometry and Ion Processes* **1997**, 169-170, (0), 217-230.
29
- 30 33. Sweeney, P. J.; Walker, J. M., Proteinase K (EC 3.4. 21.14). *Enzymes of Molecular Biology*
31
32
33 **1993**, 16, 305-317.
34
- 35 34. Guntelberg, A.; Ottesen, M., Purification of the proteolytic enzyme from *Bacillus subtilis*.
36
37
38 *Comptes rendus des travaux du Laboratoire Carlsberg. Série chimique* **1954**, 29, (3-4), 36.
39
- 40 35. Hanzawa, S.; Kidokoro, S.-I.; Flickinger, M. C., Thermolysin. In *Encyclopedia of Industrial*
41
42
43 *Biotechnology*, John Wiley & Sons, Inc.: 2009.
44
- 45 36. Fischer, D.; Wolfson, H.; Lin, S. L.; Nussinov, R., Three-dimensional, sequence order-
46
47
48 independent structural comparison of a serine protease against the crystallographic database
49
50 reveals active site similarities: Potential implications to evolution and to protein folding.
51
52
53 *Protein Science* **1994**, 3, (5), 769-778.
54
55
56
57
58
59
60

- 1
2
3
4
5
6
7
8
9
10
11
12
13
14
15
16
17
18
19
20
21
22
23
24
25
26
27
28
29
30
31
32
33
34
35
36
37
38
39
40
41
42
43
44
45
46
47
48
49
50
51
52
53
54
55
56
57
58
59
60
37. Thobhani, S.; Yuen, C.-T.; Bailey, M. J. A.; Jones, C., Identification and quantification of N-linked oligosaccharides released from glycoproteins: An inter-laboratory study. *Glycobiology* **2009**, 19, (3), 201-211.
38. Thaysen-Andersen, M.; Mysling, S.; Højrup, P., Site-Specific Glycoprofiling of N-Linked Glycopeptides Using MALDI-TOF MS: Strong Correlation between Signal Strength and Glycoform Quantities. *Analytical Chemistry* **2009**, 81, (10), 3933-3943.
39. Fu, D.; Chen, L.; O'Neill, R. A., A detailed structural characterization of ribonuclease B oligosaccharides by 1H NMR spectroscopy and mass spectrometry. *Carbohydrate Research* **1994**, 261, (2), 173-186.
40. Aldredge, D.; An, H. J.; Tang, N.; Waddell, K.; Lebrilla, C. B., Annotation of a Serum N-Glycan Library for Rapid Identification of Structures. *Journal of Proteome Research* **2012**, 11, (3), 1958-1968.
41. Catalona, W. J.; Richie, J. P.; Ahmann, F. R.; Hudson, M. A.; Scardino, P. T.; Flanigan, R. C.; deKernion, J. B.; Ratliff, T. L.; Kavoussi, L. R.; Dalkin, B. L., Comparison of digital rectal examination and serum prostate specific antigen in the early detection of prostate cancer: results of a multicenter clinical trial of 6,630 men. *The Journal of Urology* **1994**, 151, (5), 1283-1290.
42. Partin, A. W.; Catalona, W. J.; Southwick, P. C.; Subong, E. N. P.; Gasior, G. H.; Chan, D. W., Analysis of percent free prostate-specific antigen (PSA) for prostate cancer detection: Influence of total psa, prostate volume, and age. *Urology* **1996**, 48, (6, Supplement 1), 55-61.
43. Schröder, F. H.; Hugosson, J.; Roobol, M. J.; Tammela, T. L. J.; Ciatto, S.; Nelen, V.; Kwiatkowski, M.; Lujan, M.; Lilja, H.; Zappa, M.; Denis, L. J.; Recker, F.; Berenguer, A.; Määttänen, L.; Bangma, C. H.; Aus, G.; Villers, A.; Rebillard, X.; van der Kwast, T.;

- 1
2
3 Blijenberg, B. G.; Moss, S. M.; de Koning, H. J.; Auvinen, A., Screening and Prostate-
4 Cancer Mortality in a Randomized European Study. *New England Journal of Medicine* **2009**,
5
6 360, (13), 1320-1328.
7
8
9
10 44. Heidenreich, A.; Bellmunt, J.; Bolla, M.; Joniau, S.; Mason, M.; Matveev, V.; Mottet, N.;
11 Schmid, H.-P.; van der Kwast, T.; Wiegel, T.; Zattoni, F., EAU Guidelines on Prostate
12 Cancer. Part 1: Screening, Diagnosis, and Treatment of Clinically Localised Disease.
13
14
15
16
17 *European Urology* **2011**, 59, (1), 61-71.
18
19
20 45. Peracaula, R.; Tabarés, G.; Royle, L.; Harvey, D. J.; Dwek, R. A.; Rudd, P. M.; de Llorens,
21 R., Altered glycosylation pattern allows the distinction between prostate-specific antigen
22 (PSA) from normal and tumor origins. *Glycobiology* **2003**, 13, (6), 457-470.
23
24
25
26
27 46. Tabarés, G.; Radcliffe, C. M.; Barrabés, S.; Ramírez, M.; Aleixandre, R. N.; Hoesel, W.;
28 Dwek, R. A.; Rudd, P. M.; Peracaula, R.; de Llorens, R., Different glycan structures in
29 prostate-specific antigen from prostate cancer sera in relation to seminal plasma PSA.
30
31
32
33
34 *Glycobiology* **2006**, 16, (2), 132-145.
35
36
37 47. Kenny, H. A.; Kaur, S.; Coussens, L. M.; Lengyel, E., The initial steps of ovarian cancer cell
38 metastasis are mediated by MMP-2 cleavage of vitronectin and fibronectin. *The Journal of*
39
40
41
42 *Clinical Investigation* **2008**, 118, (4), 1367-1379.
43
44
45 48. Hurt, E. M.; Chan, K.; Duhagon Serrat, M. A.; Thomas, S. B.; Veenstra, T. D.; Farrar, W. L.,
46 Identification of Vitronectin as an Extrinsic Inducer of Cancer Stem Cell Differentiation and
47
48
49 Tumor Formation. *STEM CELLS* **2010**, 28, (3), 390-398.
50
51 49. Ogawa, H.; Yoneda, A.; Seno, N.; Hayashi, M.; Ishizuka, I.; Hase, S.; Matsumoto, I.,
52 Structures of the N-Linked Oligosaccharides on Human Plasma Vitronectin. *European*
53
54
55
56
57
58
59
60 *Journal of Biochemistry* **1995**, 230, (3), 994-1000.

- 1
2
3
4
5
6
7
8
9
10
11
12
13
14
15
16
17
18
19
20
21
22
23
24
25
26
27
28
29
30
31
32
33
34
35
36
37
38
39
40
41
42
43
44
45
46
47
48
49
50
51
52
53
54
55
56
57
58
59
60
50. Stübiger, G.; Marchetti, M.; Nagano, M.; Grimm, R.; Gmeiner, G.; Reichel, C.; Allmaier, G., Characterization of N- and O-glycopeptides of recombinant human erythropoietins as potential biomarkers for doping analysis by means of microscale sample purification combined with MALDI-TOF and quadrupole IT/RTOF mass spectrometry. *Journal of Separation Science* **2005**, 28, (14), 1764-1778.
51. Oh, M. J.; Hua, S.; Kim, B. J.; Jeong, H. N.; Jeong, S. H.; Grimm, R.; Yoo, J. S.; An, H. J., Analytical platform for glycomic characterization of recombinant erythropoietin biotherapeutics and biosimilars by MS. *Bioanalysis* **2013**, 5, (5), 545-559.
52. Du, Y.; Wang, F.; May, K.; Xu, W.; Liu, H., LC-MS analysis of glycopeptides of recombinant monoclonal antibodies by a rapid digestion procedure. *Journal of Chromatography B* **2012**, 907, (0), 87-93.
53. Dodds, E. D., Gas-phase dissociation of glycosylated peptide ions. *Mass Spectrometry Reviews* **2012**, 31, (6), 666-682.
54. Llop, E.; Gutiérrez-Gallego, R.; Segura, J.; Mallorquí, J.; Pascual, J. A., Structural analysis of the glycosylation of gene-activated erythropoietin (epoetin delta, Dynepo). *Analytical Biochemistry* **2008**, 383, (2), 243-254.
55. Rogers, G. N.; Herrler, G.; Paulson, J. C.; Klenk, H. D., Influenza C virus uses 9-O-acetyl-N-acetylneuraminic acid as a high affinity receptor determinant for attachment to cells. *Journal of Biological Chemistry* **1986**, 261, (13), 5947-5951.
56. Schultze, B.; Herrler, G., Bovine coronavirus uses N-acetyl-9-O-acetylneuraminic acid as a receptor determinant to initiate the infection of cultured cells. *Journal of General Virology* **1992**, 73, (4), 901-906.

FIGURES

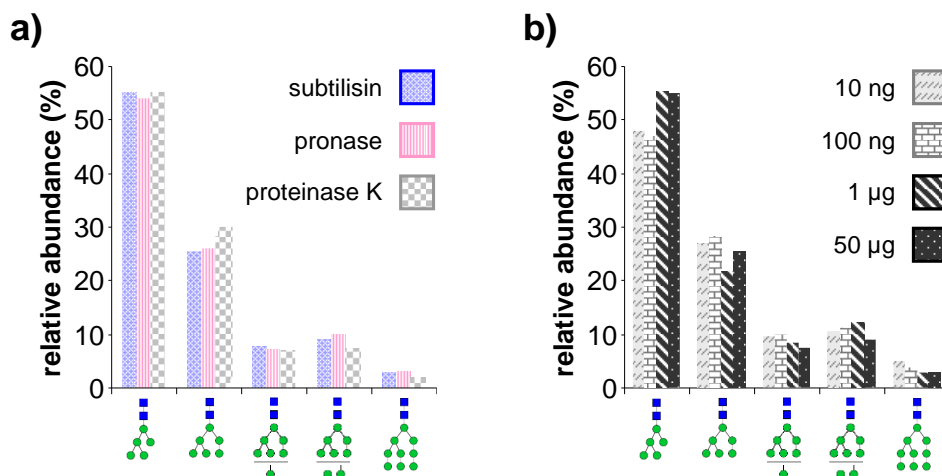


FIGURE 1: Glycoform profiles of standard glycoprotein ribonuclease B obtained following a) digestion with multispecific proteases subtilisin, pronase, and proteinase K; and b) subtilisin digestion using 50 µg, 1 µg, 100 ng, and 10 ng of initial glycoprotein.

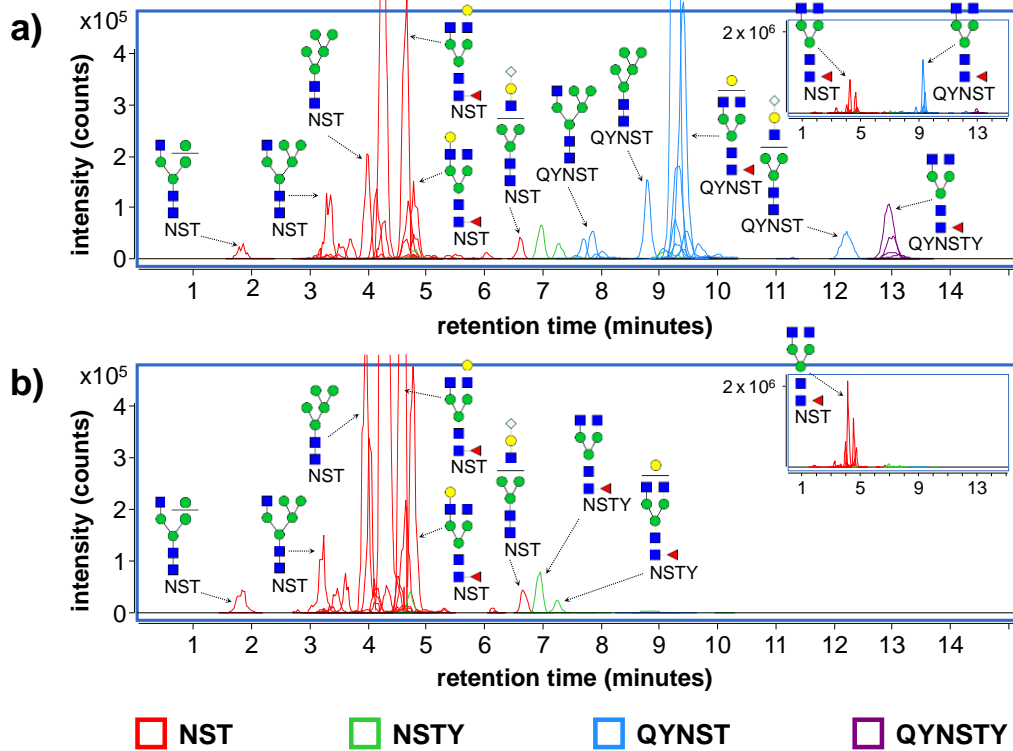


FIGURE 2: Overlaid chromatograms of glycopeptides generated by digestion of infliximab with subtilisin for a) 20 minutes, and b) 18 hours. Glycopeptide identities are confirmed by MS/MS.

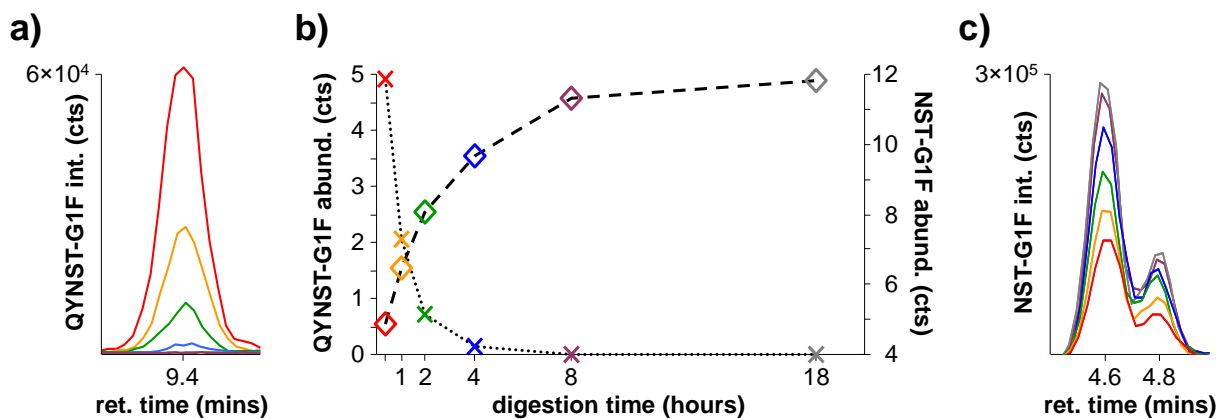


FIGURE 3: Digestion of infliximab glycoform Hex₄HexNAc₄Fuc (G1F) by subtilisin over the course of 18 hours. a) Chromatograms of QYNST-G1F decreasing in size over time; b) Plot of QYNST-G1F and NST-G1F abundances over time; and c) Chromatograms of NST-G1F increasing in size over time. Colors denote progression of time, with red marking the earliest timepoint (20 minutes) and gray marking the latest timepoint (18 hours).

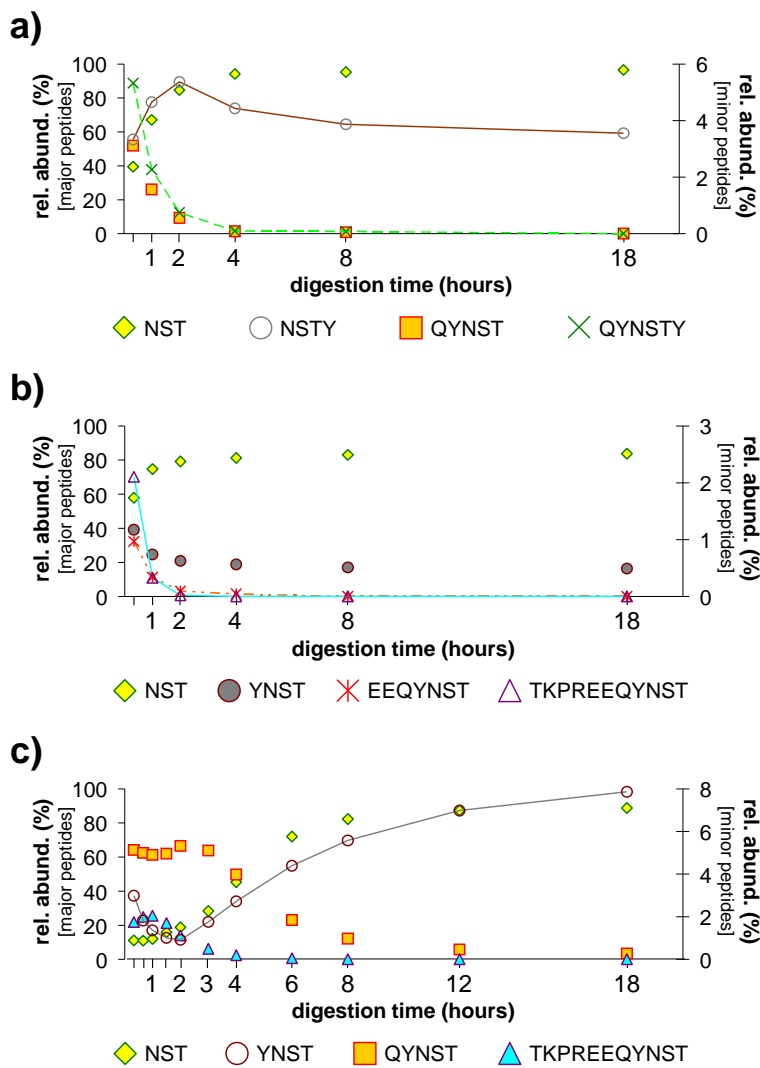


FIGURE 4: Progression of infliximab digestion by a) subtilisin; b) pronase; and c) proteinase K at different intervals over the course of 18 hours. For each digestion timepoint, the percent contributions of each peptide moiety to the overall glycopeptide population are plotted. Minor peptide moieties (right axis) are denoted by lines connected each timepoint; major peptide moieties (left axis) do not have lines connecting the timepoints.

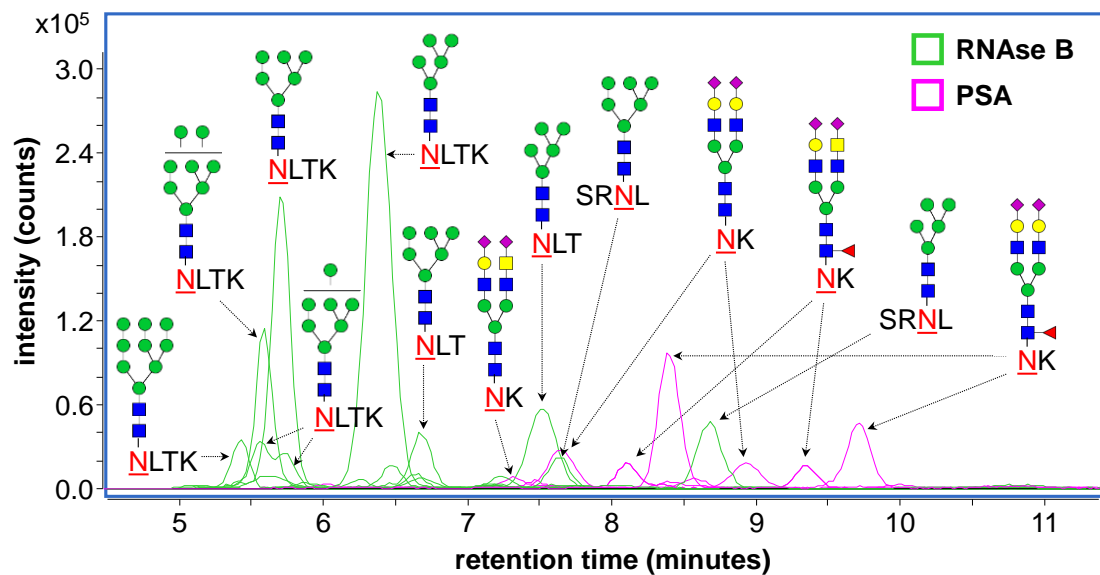


FIGURE 5: Overlaid chromatograms of glycopeptides digested by subtilisin from a mixture of RNase B and prostate-specific antigen (PSA). Glycopeptide identities are confirmed by MS/MS.

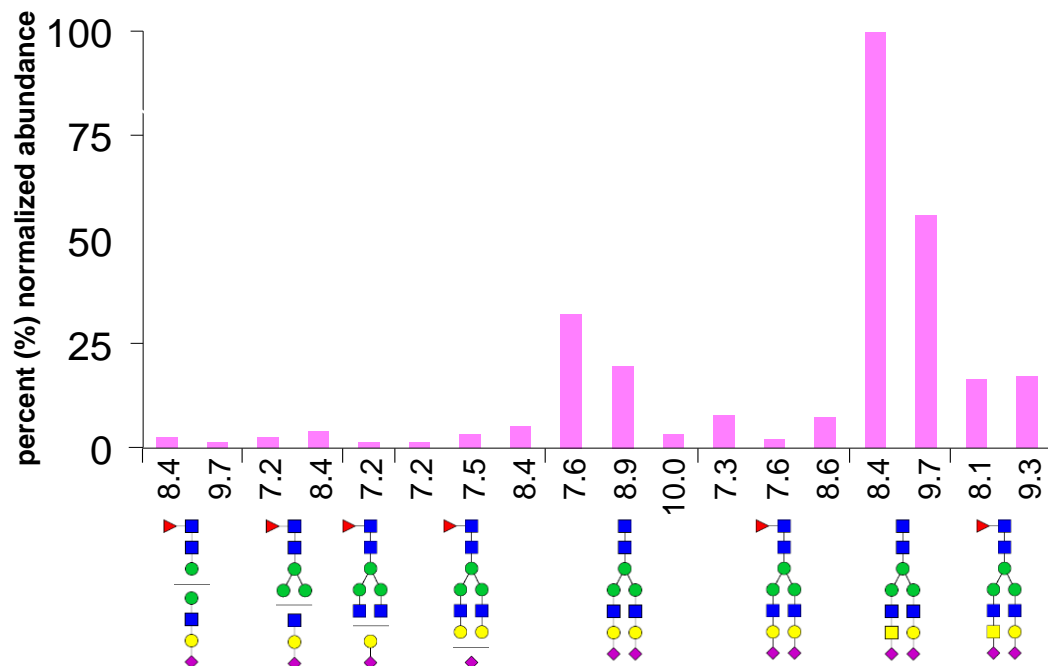


FIGURE 6: Glycoforms of prostate-specific antigen (PSA). Quantities are reported relative to the most abundant glycoform. A putative structure is suggested for each glycoform composition observed. Chromatographically-separated regioisomers are separately quantified. Retention times are reported, in minutes, for glycopeptides attached to an NK peptide moiety.

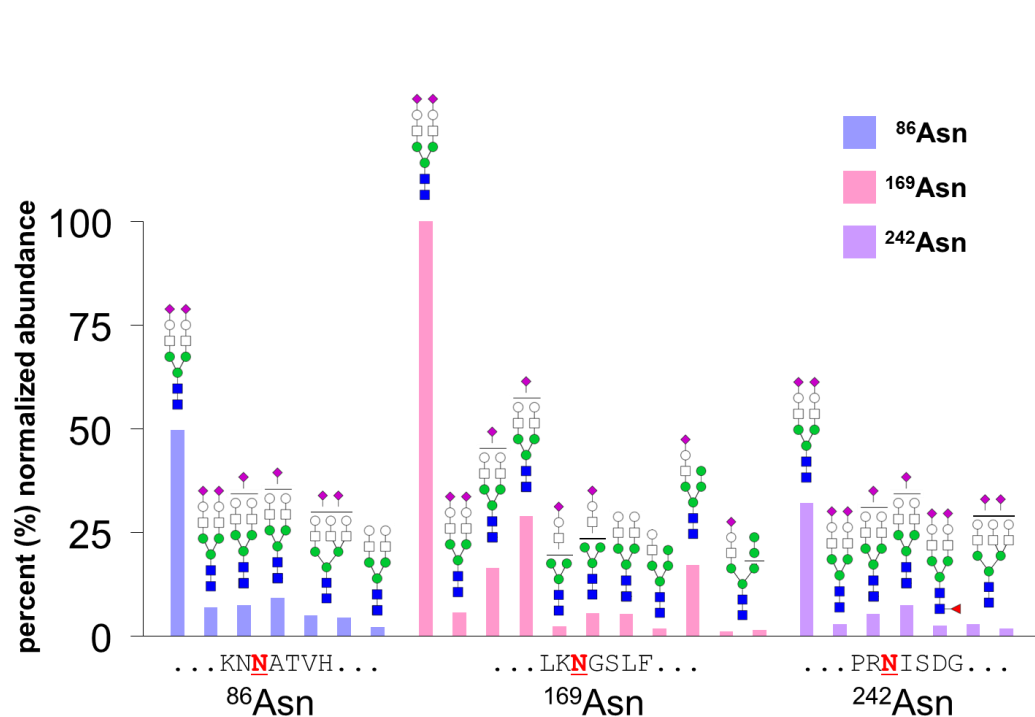


FIGURE 7: Quantitative, isomer-specific, site-specific glycosylation profile of vitronectin. Quantities are reported relative to the most abundant glycoform. A putative structure is suggested for each glycoform composition observed. Chromatographically-separated regioisomers are separately quantified. Each color represents a different glycosylation site.

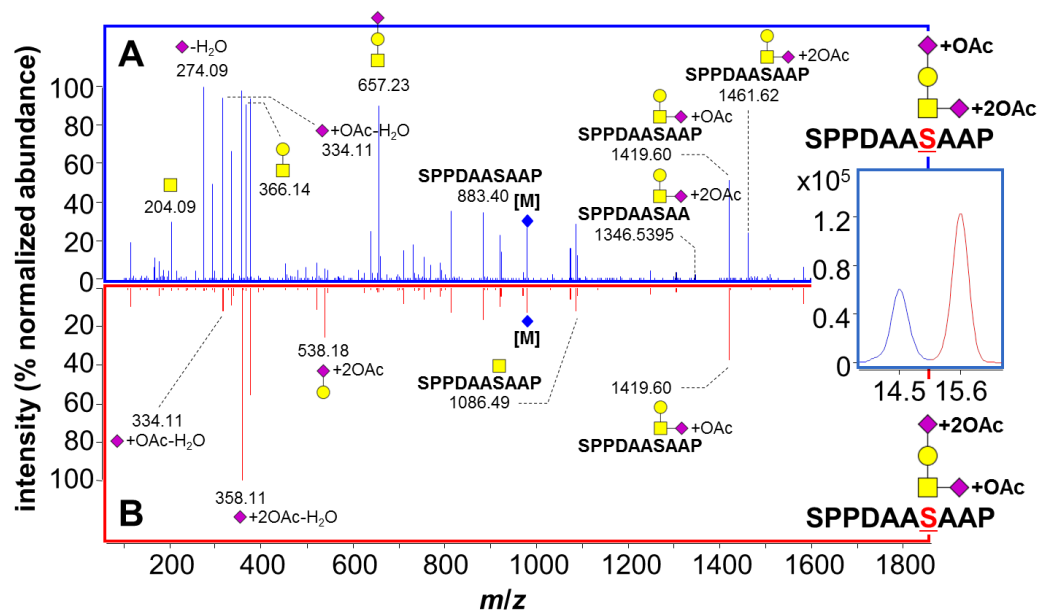


FIGURE 8: Positive ion CID MS/MS spectra of isomeric glycopeptides digested from the O-glycosylation site of recombinant erythropoietin and separated by porous graphitized carbon nano-LC. On top, a) the isomer of SPPDAASAAP+Hex₁HexNAc₁NeuAc₂+3OAc eluting at 14.5 minutes; and on the bottom, b) the isomer eluting at 15.6 minutes.

Graphical Abstract:

